Polymer Testing 93 (2021) 106935

Contents lists available at ScienceDirect

Polymer Testing

journal homepage: http://www.elsevier.com/locate/polytest

Microscopy techniques for protocell characterization

Hua Wu [a,b], Yan Qiao [a,b,*]

[a] Beijing National Laboratory for Molecular Sciences, State Key Laboratory of Polymer Physics and Chemistry, CAS Research/Education Center for Excellence in Molecular Sciences, Institute of Chemistry, Chinese Academy of Sciences, Beijing, 100190, China
[b] University of Chinese Academy of Sciences, Beijing, 100049, China

ARTICLE INFO

Keywords:
Protocell
Characterization
Microscopy
Microcompartment
Biomedical materials

ABSTRACT

Recent advances have witnessed the research progress of synthetic preliminary forms of cell-like entities (protocells) towards understanding the origin of life. Microscopy techniques have been instrumental to study protocells both in structural characterization and biomimetic functions. Advanced microscopes equipped with different illumination sources (light or electron) and detectors, have provided a versatile platform to investigate the thermodynamic and kinetic behaviors of protocells across a range of scales. Understanding the functions and advantages of each technique is a prerequisite for researchers to obtain high quality microscopic images and extract in-depth structural information. To this end, we provide a brief overview of the applications of microscopic techniques in characterizing protocells, together with discussion of their advantages and drawbacks.

1. Introduction

The mimic of cellular functions within compartmentalized synthetic cell-like entities (protocells) is a fundamental route towards the understanding of the origin of life [1], which is remaining one of the biggest questions in modern life science. Continuous efforts in synthetic protocells have led to progresses in the constructions of various compartment structures, such as fatty acid and lipid vesicles [2], polymersomes [3], proteinosomes [[4]], colloidosomes [[5]], coacervate microdroplets [6], as well as hybrid or hierarchical protocells e.g. membrane-coated coacervate microdroplets [7], protocells with organelles [8], and prototissues [9]. These synthetic protocells are capable of displaying emergent life-like behaviours and potentially contributing to the biomedical applications. From a structural characterization point of view, a combination of instrumental tools (e.g. optical microscopy, fluorescence microscopy, transmission electron microscopy, small angle X-ray scattering, dynamic light scattering and fluorescence spectroscopy) have been employed to obtain structural details in protocell research.

Among these, microscopy techniques including light microscopy, electron microscopy and scanning probe microscopy play an essential role in researching the thermodynamic and kinetic properties (e.g., morphology, size, shape transition and movement). In this Review, we first provide a brief introduction to these techniques in characterizing protocells, with particular emphasis on how to choose suitable methods for a specific purpose. We start with a systematic view of light microscopies and their recent applications with attempts beyond basic observation of the protocell shape and motility. We then summarize recent research works using electron microscopy techniques in high-resolution imaging of synthetic cells. Following this, we present a summary of using scanning probe microscopies to study various physicochemical properties such as mechanical strength, elemental composition, and magnetic performance; especially, we show that structural details of protocells with atomic-level resolution can be obtained. Beyond these discussions, some advanced or newly developed techniques such as light-sheet microscopy, spinning disk confocal microscopy, and cryogenic electron microscopy, which are currently barely explored in protocell imaging, will be referred as well. We hope this Review will provide a sketch to these microscopy techniques and hopefully accelerate the applications in researching protocell structures and their cell-like behaviours.

2. Light microscopy

In the past few centuries, microscopy techniques have been known as powerful research tools contributing to enormous ground-breaking discoveries. The invention of light microscopy (LM) has unfolded a new world in the microscale to untangle the complex mysteries of

* Corresponding author. Beijing National Laboratory for Molecular Sciences, State Key Laboratory of Polymer Physics and Chemistry, CAS Research/Education Center for Excellence in Molecular Sciences, Institute of Chemistry, Chinese Academy of Sciences, Beijing, 100190, China.
E-mail address: yanqiao@iccas.ac.cn (Y. Qiao).

https://doi.org/10.1016/j.polymertesting.2020.106935
Received 30 September 2020; Received in revised form 22 October 2020; Accepted 24 October 2020
Available online 27 October 2020

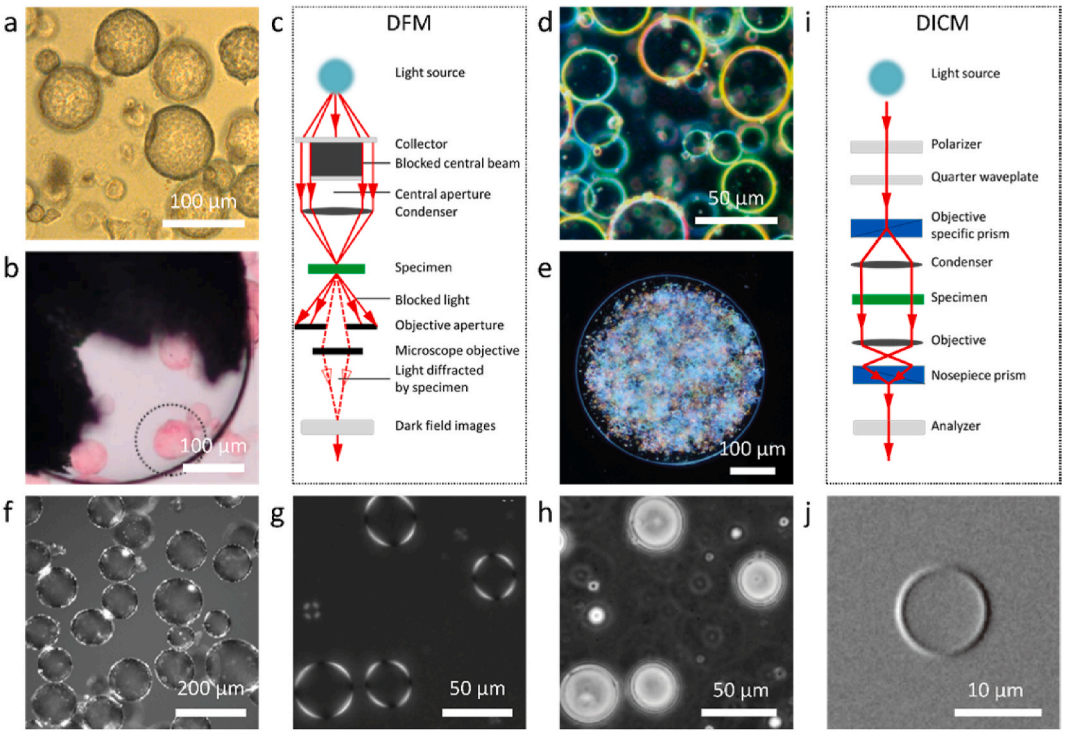

Fig. 1. (**a**,**b**) Bright field micrographs of colloidosomes. (**a**) Silica nanoparticle-bounded colloidosomes with rough surface texture. (**b**) The spontaneous capture of dye-loaded silica colloidosomes (red objects) into a magnetic Pickering emulsion droplet (black object). (**c**) Schematic illustration of DFM which collects the transmitted scattered light of specimen illuminated by a cone-shape beam. (**d**,**e**) DFM images of PCVs consisting of reconfigured coacervate microdroplets into membrane-bound vesicle-like structures in the presence of charged polyoxometalate. (**d**) PCVs vesicles with three-tiered micro-architecture consisting of a Ru_4POM/PTA/PDDA catalytic membrane-bound coacervate vesicles. (**e**) A single amino-clay/DNA membrane microcompartment containing a dense population of catalytically active Ru_4PCVs proto-organelles. (**f**) Mono-PLM image of FeM-clay colloidosomes in cyclohexane, indicating self-assembly and preferential localization of the organically modified FeM-clay at the water/oil interface. (**g**) Cross-PLM image of spherical PTA/PDDA membrane-bound coacervate vesicles where one can see strong birefringence across their surfaces. (**h**) PCM image of spherical PTA/PDDA membrane-bound coacervate vesicles. (**i**) Schematic illustration of DICM where the polarizer is directly installed in front of the condensing system, making the light linearly polarized. The light is then divided into two beams by the DIC prism, which will pass through the adjacent parts of the sample at different times, and merged by another prism, so the subtle differences of thickness in specimen can be converted into luminance difference. (**j**) DICM image of a typical giant unilamellar vesicle made of DOPC.

biology ever since the 17th century when Antoni van Leeuwenhoek and English scientist Robert Hooke first reported observations [10,11]. Over the past three centuries, technological and manufacturing breakthroughs have significantly advanced the developments of microscope designs featuring dramatically improved image quality with minimal aberration. However, the optical imaging resolution limit is determined by half the wavelength λ, the refractive index n of the medium, and the angle θ of the cone of focused light. In the research field of protocell, this effect is less profound since the size of protocells is mostly far above the resolution limit.

The development of video microscope systems enables the *in situ* image recording, which is of particular importance to understand the dynamic behaviors in natural state without invasive sample fixing and staining. Besides, the instrumental expansions to combine the LMs with well-designed fluorescent apparatus made possible to reveal the detailed inner microstructures, which are pivotal in studying hieratical complex protocells. However, it is also worth mentioned that ordinary LMs are also restricted by several shortcomings. For example, it is challenging to image the sub-cell structures as limited by its inherent microscopic magnification and resolution, although there are some technological expansions developed to alleviate the problem.

In this part, we will briefly introduce the LM techniques in three major categories based on the imaging mechanisms (i.e. the transmitted LMs, the reflected ones, and advanced techniques for protocell characterization). Application of these microscopy techniques in studying synthetic protocells with regards to their structures and functions will be discussed.

2.1. *Transmitted light microscopy*

Transmitted light microscopy (TLM) is associated for any type of microscopy where the light passes from the specimen to the opposite side of the lens. TLM measurements require the specimen to be thin and transparent for light transmission. There exist five major modes of TLM according to the imaging principles: bright field microscopy (BFM), dark field microscopy (DFM), polarized light microscopy (PLM), phase contrast microscopy (PCM), and differential interference contrast microscopy (DICM).

BFM is often used for the direct observation and video record of the size, morphology, positioning and dynamic information of the protocells in natural state. BFM is particularly useful for imaging samples that have intrinsic colour or texture, such as colloidosomes [12], which have cell-like functions such as selective permeable membrane, metabolism and gene expression [[13–15]]. These inorganic nanoparticle-bounded water-filled microcompartments have been constructed as inorganic protocells using crosslinked silica nanoparticles with average diameter of around 200 μm. The rough surface texture of resultant colloidosomes was clearly observed *via* BFM (Fig. 1a) [[16]]. Besides, the real colour imaging in BFM can also be used to differentiate protocell populations. In a binary community of synthetic protocells with artificial phagocytosis, multiple dye (carmine)-loaded silica colloidosomes (red objects) were selectively ingested by self-propelled magnetic Pickering emulsion droplets stabilized by amphiphilic colloidal iron oxide and fatty acid (black object) (Fig. 1b) [17].

DFM is a technique that relies on the transmitted scattered light but

is distinct from BFM (Fig. 1c). In DFM, a cone-shape beam formed by blocking the center of a solid light is used to illuminate the specimen, and the scattered light is collected for imaging. Accordingly, the sample appears bright while the background being dark in the image. Using this method, DFM enhances the resolution to 4–200 nm which is 50 times higher than that of BFM [18]. In this regard, DFM becomes a favored tool for protocell imaging to detect subtle structures in sub-micro scale. For example, DFM was used to visualize polyoxometalate coacervate vesicles (PCVs) which evolves from coacervate microdroplets into membrane-bound vesicle-like structures in the presence of charged polyoxometalate. Notable light scattering from nanoclusters was observed under DFM. As shown in Fig. 1d, the vesicle membranes are clearly seen indicating the incorporation of phosphotungstate (PTA) and a Ru-based polyoxometalate catalyst (Ru_4POM) into the polymer/-nucleotide membrane. The three-tiered micro-architecture consisting of a Ru_4POM/PTA/poly (diallyldimethylammonium chloride) (PDDA) catalytic membrane, a PDDA/adenosine 5′-triphosphate (ATP) sub-membrane coacervate shell, and an expanded aqueous lumen represents a synzyme protocell with catalase-like activity [19]. As clearly shown in DFM, the PCVs were encaged into an aminoclay/DNA synthetic microcapsule to form a multi-compartmentalized protocell exhibiting proto-organelle-mediated buoyancy (Fig. 1e). The outer membrane is relatively transparent due to the weak scattering of aminoclay/DNA, and the internal dense population of catalytically active Ru_4PCVs proto-organelles exhibits real colors.

PLM based on polarized light are of particular use for specimen with anisotropic structures. This endows PLMs the capability to produce the best images with a minimum optical component in the objectives. The modes of PLMs include mono-polarized and cross-polarized mode according to the number of involved polarizers. In mono-PLM where only one polarizer is used, both the morphologies and birefringent areas of specimen are observed, while in cross-PLM where two orthogonal polarizers are used, only the birefringent information would be presented. More specifically, the background under cross-PLM is dark, because there is no birefringence in the amorphous and isotropic part, and the light is blocked by the orthogonal polarizers. When the polarized light passes through the two polarization axes with a parallel direction, the birefringence parts will also appear dark, because no change of the vibration direction will occur, which makes the light unable to pass through. However, the four areas between the polarization axes appear bright as components along the vibration direction of the polarizer will form. Therefore, the whole image shows a unique black cross extinction phenomenon, which reflects the birefringence of the sample. Mono-PLM has been used in a recent work to study colloidosome protocells consisting of FeM-clay [20], which confirmed the aggregation of the organically modified clay at the water/oil emulsion interface and the birefringence phenomenon of resultant membrane (Fig. 1f). In another system of PTA/PDDA cross-linked membrane (coacervate vesicles) transformed from PDDA/ATP-enriched membrane-free coacervate droplets [21], cross-PLM was utilized to demonstrate the existence of PTA in the membrane, in which the image showed strong birefringence across the membrane surface regions (Fig. 1g).

The above microscopic techniques are based on their capabilities to absorb, scatter, or deflect the transmitted light. However, when the samples are overly thin and transparent, they do not absorb enough light and therefore it is difficult to observe them. To address this issue, extra optics that allows the phase shift of light are placed. The most common microscopy with phase shift is PCM, which is based on different refractive index and thickness of samples. PCM has a special objective that can translate the phase differences of transmitted light into visible amplitude or brightness changes, and display the structural information on a gray background. As shown in Fig. 1h, PCVs of PTA/PDDA membrane-bound coacervate vesicles can be noted as discrete spheres, showing three-tiered micro-architectures consisting of a PTA/PDDA membrane, a PDDA/ATP sub-membrane shell, and an aqueous-filled lumen (Fig. 1h) [21]. However, the complexity of PCM objective

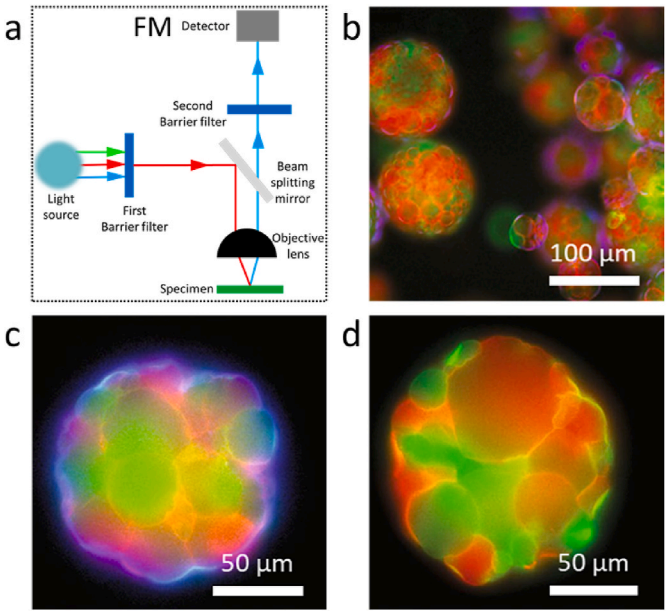

Fig. 2. (**a**) Scheme of FM. FM can easily gain an insight into the inner structure and tracking the dynamic behaviours of protocells with specified fluorescent dyes labeling. FM is widely used in biological systems, mainly because of its high sensitivity and high specificity. (**b-d**) FM images of w/o/w emulsion droplets consisting of caged multi-compartmentalized spheroids containing different proteinosomes dispersed in oil and incarcerated within a host proteinosome membrane (blue) (**b**), caged spheroid after removal of the encapsulated oil (**c**), uncaged spheroid after removal of the outer proteinosome membrane (**d**).

makes it difficult to increase the number of apertures, which limits the axial resolution. In addition, a notable halo will appear at the boundary where the refractive index varies significantly and the obscured outer edge of specimen occurs.

DICM offers a new tool to address these problems by producing high contrast images without affecting the amplitude of illumination light. Normally, the gradients of optical path length are primarily responsible for introducing image contrast in DIC microscope; while PCM relies on the optical path length of specimen. In addition, polarized light is utilized in DICM for illumination, which is further split into two beams when firstly passing through the prism, then merged when passing the prism at the second time. In this case, halo is largely absent and the pronounced differences of refractive index between specimen and surroundings are favorable for generating excellent images in DICM (Fig. 1i). DICM can display the tiny difference of thickness and create the 3-dimensional relief of imaged specimens due to the interference-derived contrast [22]. Therefore, quantitative DICM image analysis software has been developed for the measurement of giant vesicle (GV) lamellarity (the thickness of a membrane bilayer) in a rapid, noninvasive and reproducible way [23]. For example, DICM image of GVs made of DOPC (1,2-dioleoyl-3-sn-glycero phosphatidylcholine) with electro-formation method is shown in Fig. 1j. The thickness was acquired by averaging over the 128 images for noise reduction followed by the combination with equation calculation to obtain the lamellarity information.

Overall, TLMs without phase contrast or DIC are usually sufficient to observe the general morphology of protocells. Nevertheless, PCM and DICM are necessary to achieve high-contrast bright field images with more details when it comes to protocells with thin surface membranes or multiple internal microstructures (such as organelles and multilayers) that possess a distinct refractive index.

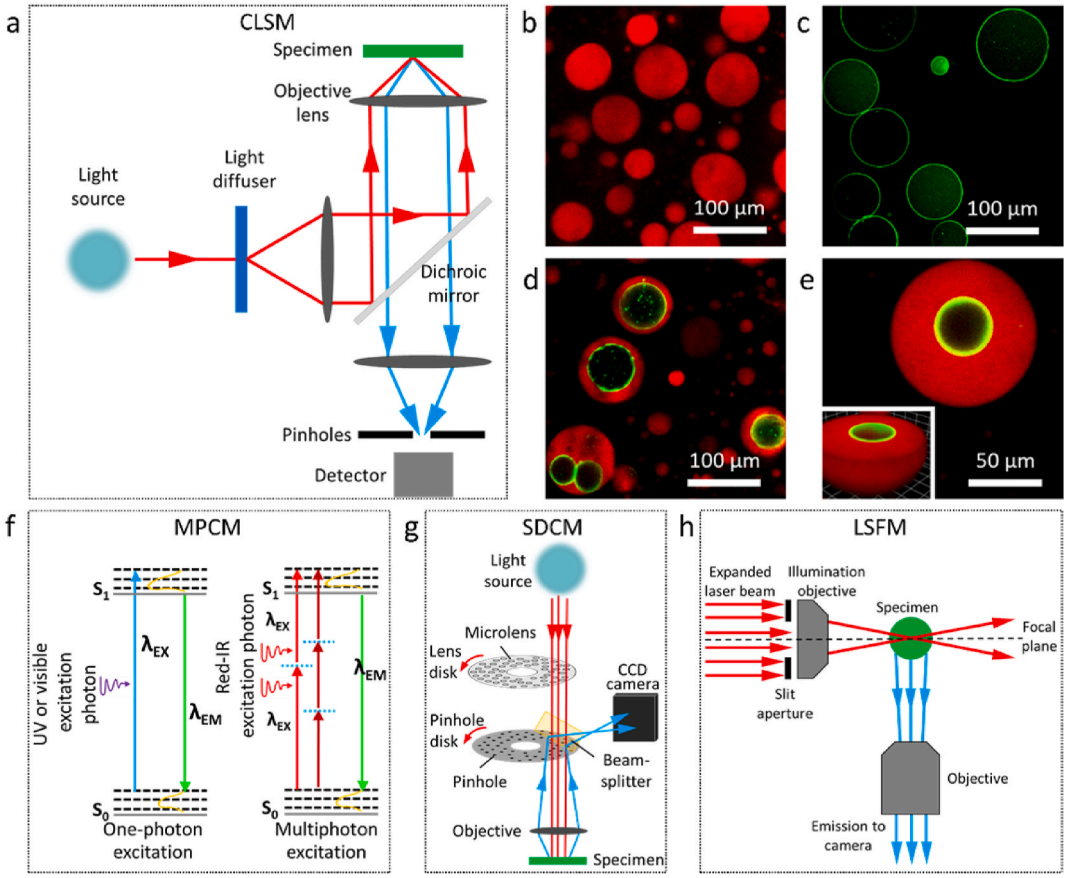

Fig. 3. (**a**) Confocal laser scanning microscope (CLSM) overview and (**b-e**) CLSM images of multi-compartmentalized protocells. (**b**) Myristic acid/guanidinium micelle coacervate droplets doped with Nile Red. (**c**) GOx-containing FITC-labeled proteinosomes. (**d**) Host–guest protocells prepared by mixing the proteinosomes and coacervate droplets at a number density ratio of 1:12. (**e**) 3D CLSM image of a single host–guest protocell. Schematic drawing of (**f**) MPCM, (**g**) SDCM and (**h**) LSFM.

2.2. Reflected light microscopy

Reflected light microscopies (RLMs) take use of reflected light for imaging and have no requirement of the specimen transparency which can significantly reduce the phototoxicity. The sub-groups of RLMs include: 1) LM in reflection mode, 2) PLM in reflection mode and 3) fluorescence microscopy (FM). The first two groups are similar to the corresponding type in TLMs except for using reflection light path. They are advantageous in characterizing opaque specimens, of which the microstructure cannot be imaged by TLMs [24]. Thus, one potential application of RLM may be found in study protocells with opaque membrane or structures susceptible to light damage. Besides, FM can be used to determine the localization and interaction of molecule species inside protocells. Intra- and intercellular processes like endocytosis and exocytosis can also be observed.

FM has been widely applied in imaging protocells since they can provide more structural details that are not readily available in other traditional optical microscopies, such as higher resolution as well as the collection of images in multiple colour channels. FM is used in the characterization of protocells such as the integrity [25], distribution and location of internal chemical substances [26], the transport (transfer) and reaction (digestion) of specific substances [27]. Through the use of multiple fluorescence labeling either by genetically encoding fluorescent proteins or by covalently binding to targeted molecules, different structures or populations can be identified simultaneously (Fig. 2a). For an instance, Mann and coauthors investigated the structure of the multi-compartmentalized spheroids (prototissues), which is a nested arrangement of water-filled bio-orthogonally reactive proteinosomes that were closely packed, dispersed in an encapsulated oil phase and housed within a bio-orthogonally non-reactive host proteinosome. The inner populations are azide-functionalized and alkyne-functionalized proteinosomes, while the host is non-bio-orthogonally crosslinked proteinosome, labeled with rhodamine isothiocyanate (RITC), fluorescein isothiocyanate (FITC) and Dylight 405 respectively (Fig. 2b) [9]. Afterwards, the removing the outer membrane or the encapsulated oil either exhibited no change in structural integrity (Fig. 2c) or trigger a bio-orthogonal ligation (Fig. 2d). In addition, more investigations such as colocalization, detection of ion concentrations, endocytosis and exocytosis in protocell systems can be realized with fluorescence microscopy.

2.3. Advanced techniques for protocell characterization

In spite of wide applications of the above-discussed microscopy techniques, advanced imaging techniques capable of multidimensional imaging, excitation damage reduction, high-resolution imaging and multifunctional analysis are still required. Recently, specialized series of newly developed microscopy techniques have been proposed to uncover the structural details of protocells.

In this section, we briefly introduce four kinds of techniques developed to acquire multidimensional imaging with reduced excitation damage, namely confocal laser scanning microscopy (CLSM, high resolution and 3D imaging), multiphoton confocal microscopy (MPCM, excellent optical sectioning ability in 3D observation and minimal damage to specimen), spinning disk confocal microscopy (SDCM, improved acquisition speed and reduced excitation damage) and light

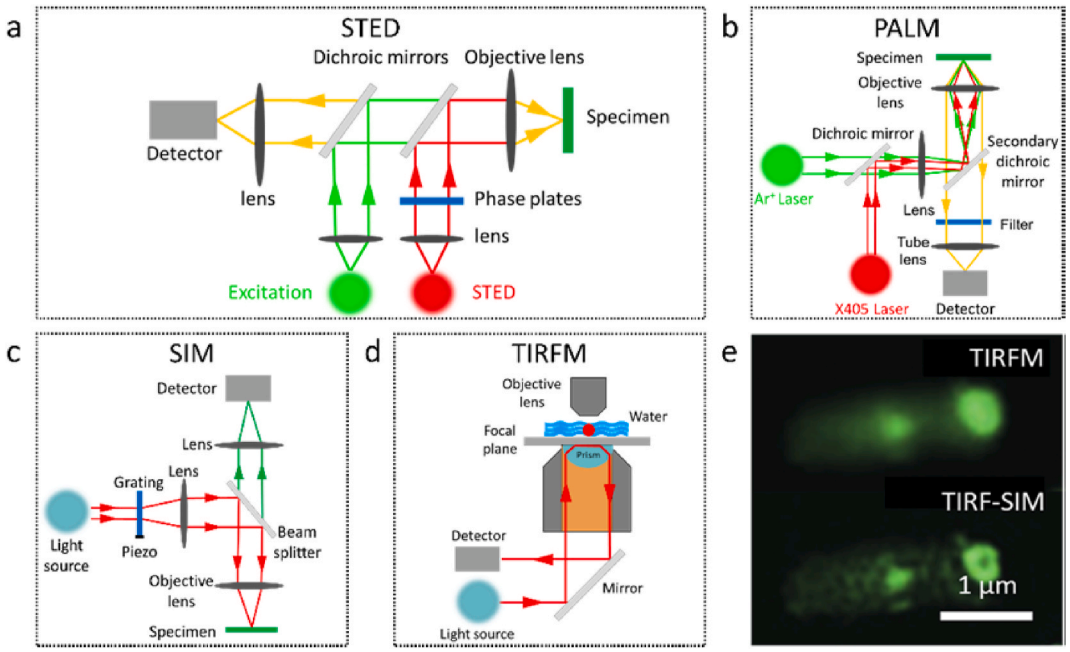

Fig. 4. Schematic drawings of (**a**) STED, (**b**) PALM, (**c**) SIM and (**d**) TIRFM. (**e**) TIRFM and TIRF-SIM images of living E. coli with artificial organelles.

sheet fluorescence microscopy (LSFM, slight photobleaching, phototoxicity and long-time 3D observation).

It remains challenging for conventional fluorescence microscopy to image subtle or 3D structures of protocells. This can become even worse for thick or densely-stained specimens due to the strong light scattering from the non-focal planes. Using point-by-point illumination and spatial pinhole modulation, the technique of CLSM is able to eliminate the disturbing scattering and improve the optical resolution and visual contrast (Fig. 3a) [28]. Meanwhile, with the assistance of moving lens system, CLSM becomes feasible to achieve a controlled scanning of the investigated specimens so that a well-resolved 3D image can be effectively acquired. Furthermore, CLSM has been extensively used for studying both static [29] and dynamic [30] behaviours of protocell models such as the multi-compartmentalized host-guest protocells. A process of spontaneous phagocytosis of proteinosomes by coacervate droplets was monitored by CLSM [31]. Fig. 3b showed discrete droplets with a uniformly distributed red Nile Red fluorescence and diameters between 5 and 200 μm. GOx-containing FITC-labeled proteinosomes can also be visualized as a spherical, non-aggregated membrane-bounded microcompartments (Fig. 3c). After the capture of proteinosomes by coacervate droplets, green fluorescence proteinosome nested red coacervate droplets were observed (Fig. 3d). Furthermore, a high-resolution 3D image captured by CLSM (Fig. 3e) provided an intuitive illustration of hierarchical structures of multi-compartmentalized protocells. However, due to the point-by-point scanning mode, a fleeting light irradiation time of each point leads to the low quantum efficiency of the imaging sensor, therefore strong excitation energy was required in CLSM to achieve sufficient imaging speed, causing relatively serious photobleaching and phototoxicity.

To avoid the phototoxicity, MPCM with near-infrared laser illumination has been explored (Fig. 3f) [32,33]. Nowadays, two-photon technique stands as the mainstream [34] due to several main reasons. First, two photon lasers with longer wavelength and lower energy can better penetrate tissue to excite fluorophores. Second, the use of two-photon laser to excite fluorophores can largely avoid self-fluorescence from tissue components (e.g., proteins). Third, two-photon microscope only excites fluorophores in the right plane, which reduces unnecessary bleaching of fluorophores. Moreover, the two-photon excitation provides excellent optical sectioning mainly used for living cells and bio-tissues, which shows great potential in protocell-based tissue observation [9].

To achieve the dynamic imaging, spinning disk systems have been developed. In SDCM, image detection is restricted to a focal plane by an array of pinholes in a rapidly spinning disk (Fig. 3g). The pinholes also distribute laser excitation. Therefore, SDCM can realize a multi-point synchronous scanning to decrease the photobleaching and improve the acquisition speed. Furthermore, SDCMs are also capable of multidimensional image acquisition. All these merits lead to the widely adoption of SDCM in 3D imaging, fast dynamic imaging, long time series shooting and internal detail structure imaging [35–38]. For the application of SDCM in coacervate-based protocells, the quick engulfment of core coacervates (ATP/poly(allylamine hydrochloride)) into the outer coacervate phase (poly(3-sulfopropyl methacrylate)/PDDA) and resultant multi-phase coacervate droplets were clearly observed, which further demonstrates the fast and high-resolution imaging of SDCM and its potential applications on protocell characterization [39].

LSFM (also known as single plane illumination microscopy) exhibits superiority on fully enhanced abilities over large field visualization, low acquisition duration, high resolution, high imaging speed, low light damage and long-time observation, as well as excellent signal-to-noise ratio yielding. As shown in Fig. 3h, by illuminating with an ultra-thin single light plane generated by two intersected lasers, 3D imaging of relatively large specimens can be realized [40]. In this way, only light from the focal plane will be detected, and the out-of-focus light can be neglected. Furthermore, the orthogonal arrangement of objective and detector decouples the illumination and detection, thus enables intrinsic 3D optical sectioning [41]. The application of LSFM ranges from the imaging of subcellular structures, rapid inter- and intracellular processes to the acquisition of long-term processes, as well as the visualization of complete specimen.

3. High-resolution imaging

Due to the diffraction limit of light, it is challenging to visualize ultrastructure with light microscopy. To realize high-resolution imaging, super resolution microscopy has been developed to overcome the diffraction limit of light and thus allow ultrastructure imaging. Super resolution techniques use a variety of methods to break the diffraction

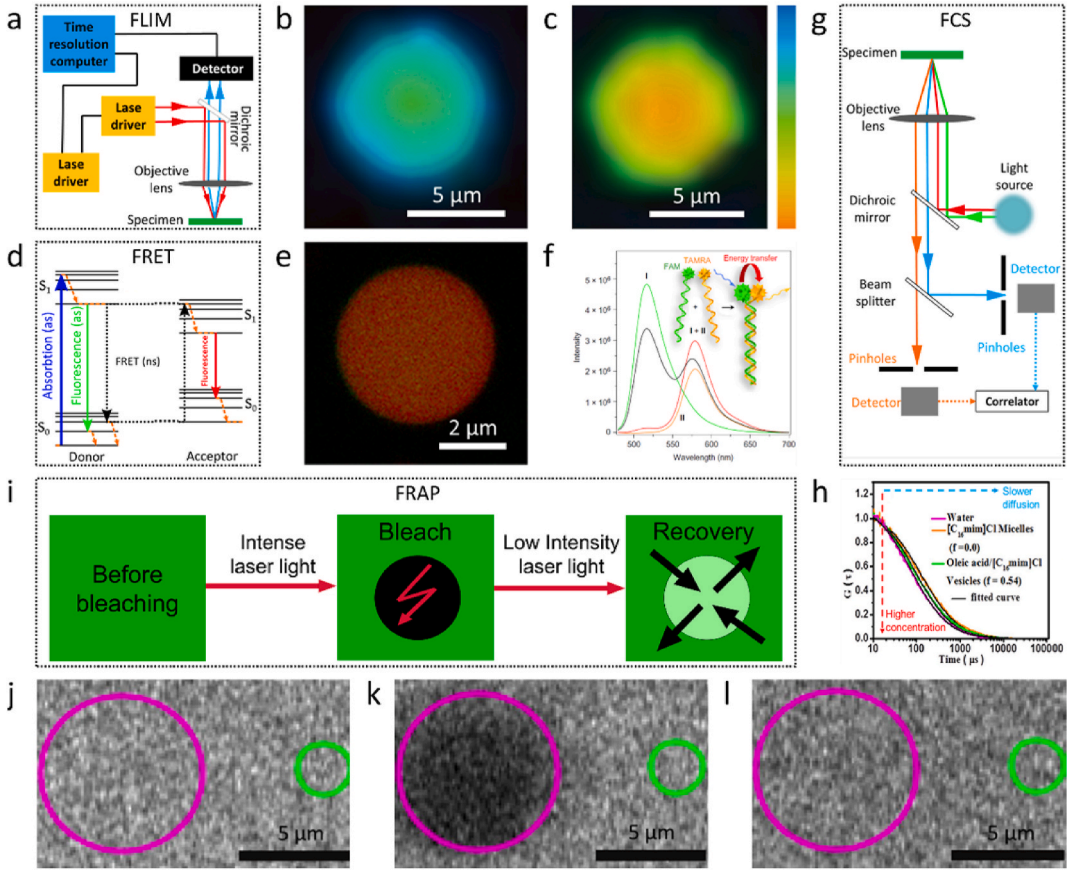

Fig. 5. Schematic illustrations of (**a**) FLIM, (**d**) FRET, (**g**) FCS, (**i**) FRAP, respectively. (**b,c**) Fluorescence lifetime maps for oleate/PDDA/ATP microdroplets that contain kiton red (**b**) in the absence or (**c**) presence of NaCl. (**e**) Fluorescence microscopy image of a green/red superimposed image of coacervate microdroplets containing FAM-ssDNA and TAMRA-ssDNA with FRET phenomenon. (**f**) Fluorescence emission spectra recorded on dispersions of coacervate microdroplets containing FAM-ssDNA (I, green plot) or TAMRA-ssDNA (II, orange plot), or both with FRET phenomenon (I + II) (red plot). (**h**) FCS spectrum for dye diffusion coefficient measuring. (**j-l**) FRAP of bulk coacervate phase containing TAM–HH–min.

limit of light: stimulated emission depletion technique (STED, based on stimulated emission quenching), photoactivated localization technique or stochastic optical reconstruction microscopy (PALM/STORM, based on single molecule imaging and localizing) and structured illumination microscopy (SIM, based on structured light illuminating). Besides, total internal reflection fluorescent microscopy (TIRFM, based on the evanescent wave generated on the other side of medium after total reflection of light) was also an effective way to achieve high-resolution imaging.

STED breaks the light diffraction limit and realizes a resolution of ~50 nm. Similar to CLSM, STED image is gained by an excitation laser beam with a pinhole to remove out-of-focus light (Fig. 4a). The resolution enhancement relies on the concomitant illumination from a second laser [42]. The second laser with a red-shifted emission wavelength can quench peripheral excited fluorophores by stimulated emission depletion. Therefore, the resolution of the STED system can be improved by considering the fluorophore as an active element but not as a simple reporter during the acquisition process.

Different with STED imaging, PALM/STORM image the sample by repeatedly exciting and capturing of a single or several fluorescent molecules (Fig. 4b) [43]. This process is repeated for thousands of times on different subsets of molecules to obtain the super-resolution image (resolution reaching 20–50 nm) [44,45]. Despite the high spatial resolution achieved by PALM/STORM, some disadvantages still exist, such as strong excitation light requirement for irradiation, which will result in serious photobleaching and phototoxicity.

Furthermore, SIM can effectively utilize the emitted photons and greatly lower the requirements on fluorescent molecules. By superposing a well-defined grating, SIM can achieve the spatial structure regulating of excitation beam, which will excite the hybrid frequency of the grating and fluorescence density (Fig. 4c). The high-frequency information of samples can be carried to a low-frequency band when changing the direction and phase of the grating. Therefore, the high-frequency signal can be extracted for super-resolution visualization [46]. During the past decade, SIM has been widely used in the researches of cell physiology, cell dynamics and protein co-localization. Besides, 3d-SIM can obtain images at different longitudinal levels and reconstruct 3D images by gaining a series of tomographic images.

TIRFM is also applicable for high-resolution imaging based on the high contrast obtained from the total internal reflection of fluorescence. The reflection process generates evanescent wave on the other side of reflecting plane, which can greatly reduce the background light noise (Fig. 4d). TIRFM is especially used for the single protein dynamics research on cell membrane [47], calcium detection [48], drug tracking [49] and subcellular structure imaging [50]. For example, the formation of proto-organelles by genetically encoded amphiphilic proteins was achieved in E. coli [51]. TIRFM was applied to visualize these resultant compartments and the results showed that the proto-organelles appeared as concentrated fluorescent spots of different size (Fig. 4e top). However, the TIRFM image remained too blurry, TIRF-SIM (combination of TIRFM and SIM) was then introduced for a further improvement of image resolution. In TIRF-SIM image, a few clearer and brighter fluorescent spots were observed (Fig. 4e down), revealing a ring-like substructure with an inner diameter of about 650 nm.

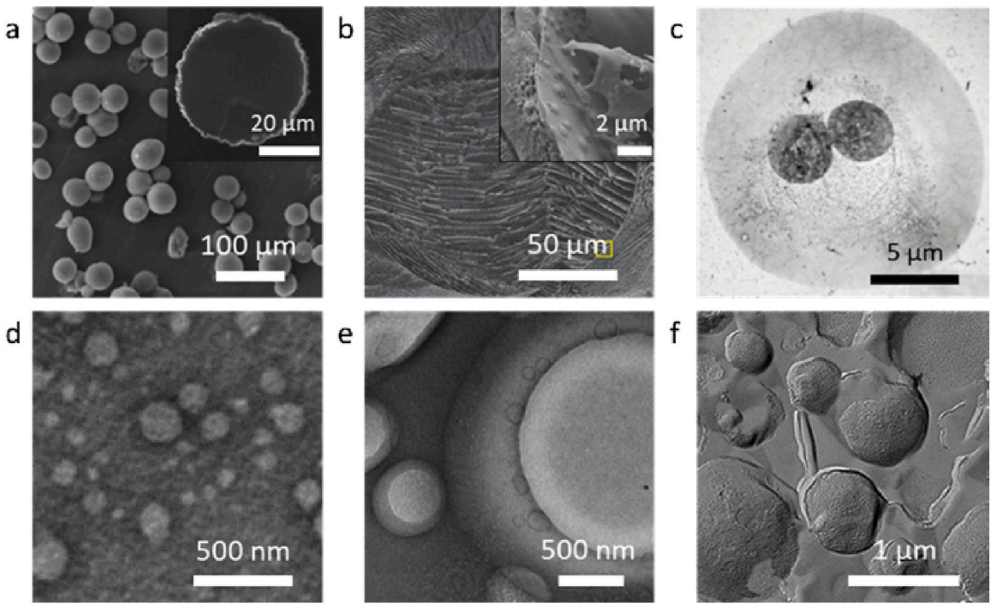

Fig. 6. (**a**) SEM micrograph of dried intact FeM-clay colloidosomes. (**b**) Cryo-SEM image of a frozen polymeric vesicle in ice. (**c**) TEM image of a two-tiered BSA-NH_2/PNIPAAm proteinosome comprising two entrapped smaller proteinosomes. (**d**) NS-TEM image of SDS and SDBS vesicles. (**e**) Cryo-TEM image of the lamellar Lα phase for the myristic acid/CsOH/H_2O system at 25 °C, showing the existence of size enlargement among the resultant vesicles. (**f**) FF-TEM image of faceted vesicles formed by perfluorononanoic acid.

4. Multifunctional analysis

A majority of the above techniques relies on fluorescence, which has revolutionized microscopy imaging in biology. While the resultant images offer merely visual information. In order to obtain further information beyond images, multiple functional analyzing systems are built such as fluorescence lifetime imaging microscopy (FLIM, monitoring the fluorescence lifetime), fluorescence resonance energy transfer (FRET, analyzing fluorophore interactions), fluorescence correlation spectroscopy (FCS, analyzing the fluorescence fluctuations) and fluorescence recovery after photobleaching (FRAP, measuring the fluorescence molecular motion), and high content analysis (HCA, automated high-throughput microscopic imaging and big data quantitative analysis).

FLIM is a technique to determine the excited state lifetimes of luminophores by means of fluorescence microscope. By monitoring the fluorescence lifetime, FLIM can provide concentration-independent information on local microenvironment (Fig. 5a). Fluorescence lifetime is independent of fluorophore concentration, which makes FLIM less susceptible to defects caused by non-uniform illumination, light path-length, scattered light, photobleaching or excitation intensity variations. FLIM has also been applied to analyze the physical environment of the fluorophore. For example, hybrid protocells consisting of coacervate microdroplets with fatty-acid membrane were constructed. Under high ionic strength, the oleate-coated polyelectrolyte/ribonucleotide droplets would appear internalized disassembly with retention of the oleate membrane [25]. FLIM was applied to evidence the internalized disassembly process and the results showed a remarkable reduction in the fluorescence lifetimes owing to the reduction in the viscosity of the compartmentalized medium (Fig. 5b and c).

FRET is a distance-dependent nonradiative energy transfer interaction between two electronic excited states of fluorescent molecules, which is a useful tool for characterizing the molecule properties in protocells (Fig. 5d). A typical FRET example in protocell research is for the investigation of artificial form of predatory behavior in synthetic protocell communities (coacervates as predator and proteinosomes as prey) [52]. The encapsulated carboxyfluorescein (FAM) modified-ssDNA and carboxytetramethylrhodamin (TAMRA) modified-ssDNA payloads encountered and paired with FRET phenomenon when the predation process happens. As shown by fluorescence image in Fig. 5e, weak green and red fluorescence in the filtered images (not shown in this paper), as well as a yellow image by overlaid red/-green channels can be seen. This was associated with FRET behaviour between double-strand hybridization of FAM-ssDNA and TAMRA-ssDNA. The FRET behaviour was further confirmed by the fluorescence spectra, indicating the 520 and 583 nm peaks were quenched and increased, respectively (Fig. 5f).

FCS is developed based on a correlation analysis of temporal fluctuations of fluorescence intensity in samples (Fig. 5g), offering an access to the diffusion behaviour and concentration variation. In this way, important biochemical parameters such as the concentration and size of detected molecules as well as viscosity of the environment can be obtained. For example, FCS was applied to study a spontaneous micelle-vesicle transition and its dynamic process in a vesicle-based system containing oleic acid and 1-hexadecyl-3-methyl imidazolium chloride (Fig. 5h) [53]. The results revealed that the spontaneous micelle-vesicle transition was accompanied by changes in the velocity of diffusional motion, and higher diffusion coefficient was acquired in vesicle state. FCS is also applied to measure the binding interactions, dynamics of cellular structures and oligomerization and single molecule spectroscopy, suggesting the potential on tracking molecular dynamics in protocell systems with FCS.

FRAP is also a powerful tool for lateral diffusion measurement, measured by confocal microscopy. Photo bleaching and recovery are carried out by irreversibly quenching a specific area and monitoring the recovery of fluorescence intensity (Fig. 5i). Recently, FRAP was applied to investigate the diffusion of ribozyme and substrate in the interior of bulk coacervate phase [54]. The resultant images showed the significant slowdown of molecular diffusion for the ribozyme and substrate in coacervate phase, compared to the predicted diffusion coefficients of RNA in buffer (Fig. 5j-l). FRAP was also employed in studying the membrane fluidity and protein/lipid group mobility [55–57].

HCA is developed for the analysis of multicellular structure and protein localization, which integrates high throughput screening technologies with advanced cellular imaging [58]. In HCA, the bright field/fluorescence microscopic acquisition, multiple-target molecule expression, temporal/spatial information, morphological information can be obtained simultaneously. Through high content image analysis software, the obtained data can be comprehensively analyzed to provide novel systems-level insight into complexed cell/protocell populations.

Light microscopy has become a powerful tool in visualizing nanoscale structures after more than 300 years' development. However, the resolution of most LM is still greatly restricted by the diffraction limit (half of the wavelength of incident light, $>$ 200 nm), though SPMs and TIRFM have made some progresses. Thus, advanced techniques that can

enable higher-resolution imaging is highly desirable.

5. Electron microscopy

Electron microscopy (EM) uses electron beams as a probe to illuminate samples and achieve much higher spatial resolution than light microscopy, bringing resolution into the level of 2 nm. Generally, electron microscopies can be classified into scanning electron microscopy (SEM) and transmission electron microscopy (TEM), which provide versatile methodologies for the characterization of micro-/nanostructures in 2D and 3D materials.

In SEM, a fine electron beam interacts with the surface of samples, which produces secondary electron (SE). The SE signal is detected by the detector and displayed on the screen of a cathode ray tube. SEM is initially used for the characterization of pollens, viruses, or cells, and gradually find their applications in many fields including protocells [59–61]. In the previous-mentioned Fe-clay colloidosome system, SEM was employed to investigate the morphology of inorganic protocells. SEM imaging of the dried or freeze-fractured colloidosomes (Fig. 6a) showed the structural robustness of individual microcapsules under vacuum, and a continuous clay membrane containing a hollow interior. The membrane of inorganic colloidosome was several micrometers in thickness with a rough surface (Fig. 6a inset) [20]. Furthermore, SEM can also be used for elemental analysis with the integration of electron energy spectrometer (EDS) [62].

However, SEM observation requires the samples to be pre-dried and completely desiccative. The dehydration process will distort the morphology of some samples especially soft organic materials. Besides, to obtain high resolution images, surface spray plating is usually employed to enhance the secondary electron yields which can increase the contrast of imaging. However, the deposition of metal layers can significantly change the surface information or even produce artifacts. This sample preparation process can cause significant structural distortion to protocell specimen, including vesicles, coacervate droplets, and proteinosomes. Therefore, cryogenic SEM (Cryo-SEM) was developed to characterize these hydrated and electron beam sensitive samples by using rapid freezing and freezing transfer systems. Cryo-SEM has been used for the observation of subtle structures in protocells. For example, Cryo-SEM was applied to visualize polymeric vesicle protocells consisting of amphiphilic block copolymer (poly (n-butyl methacrylate)94-block-poly-(N, N-dimethyl-amino ethyl methacrylate)) [63]. Cryo-SEM images can provide solid proof to confirm the embedding of manganese oxide particles inside the vesicular membranes (Fig. 6b).

Advanced SEMs such as serial block face SEM (SBF-SEM) and automatic tape collection ultrathin microtome continuous section SEM (ATUM-ssSEM) are also developed. SBF-SEM has an ultramicrotome inside of the vacuum chamber which can remove the serial sections from the block face by sequential sectioning, and the backscattered electrons from the newly formed surface can be collected to generate SEM images [64]. In this manner, as each image stays in an exact registration, a serial section movie and large-scale 3D image set can be created. ATUM-ssSEM can offer high resolution imaging due to the ability of collecting hundreds to thousands of sections on a continuous tape [65].

Although SEM remains a powerful tool, it only provides information from sample surfaces which makes it difficult to access the interior structures of specimen. To address this issue, TEM an alternative tool to study the micro-/nano-structures imaging. In TEM, a focused beam of energetic electrons transmits through a thin specimen. Depending on electron-matter interaction, the electrons can be scattered, reflected or transmit through samples. The transmitted electron can generate patterns on a fluorescent screen of image-recording system. As shown in Fig. 6c, TEM imaging revealed both the surface and internal information of proteinsomes, which is made of bovine serum albumin (BSA-NH_2)/poly(N-isopropylacrylamide) (PNIPAAm) protocell membranes. The multi-compartmentalized protocell comprised two or three levels of organized and controlled guest proteinosomes, which are regarded as chemically and spatially integrated proto-organelles [66]. TEM was employed to directly demonstrate the multi-compartmentalized structure. A collapsed but structurally intact nested microarchitecture with two entrapped proto-organelles can be clearly seen.

Soft organic materials are usually composed of light atoms such as carbon, oxygen, nitrogen and hydrogen, which can only weakly interact with electrons. As a consequence, TEM imaging of these samples cannot provide enough contrast. To address this issue, technique of negative staining (NS) was developed and applied for TEM sample preparation. The main idea of NS-TEM is coating the surface of specimen with a thin layer of electron dense material (such as phosphotungstic acid and uranyl acetate) to provide high image contrast. This technique provides structural information such as shape and size. NS-TEM has been widely used for virus imaging for a long period time, and recently has been applied in characterizing protocell models especially vesicle-based systems. As shown in Fig. 6d, the morphology of sodium dodecyl sulfate (SDS) and sodium dodecylbenzenesulfonate (SDBS) vesicles were clearly visualized [67]. However, it is also worth mentioning that the staining with heavy metal ions and the drying process during the negative staining process may bring severe artifacts.

Cryogenic TEM (Cryo-TEM) was developed to study the structures of soft nanomaterials without using metal staining process. The Cryo-TEM sample is frozen and viewed in a very cold liquid refrigerant in order to preserve and protect it during observation. Liquid ethane is used in the freezing process to make it quick enough to prevent the frozen water from forming cubic ice. In this process, the samples can remain hydrated states, which is especially important to biological macromolecules (e.g., DNA and protein). To investigate the formation of bilayer structure in fatty acid/soap mixtures, Cryo-TEM was applied to demonstrate the difference between the microstructures of vesicles formed by soap and various fatty acid including decanoic acid, lauric acid, myristic acid, palmitic acid and stearic acid. Fig. 6e showed the vesicles formation in the myristic acid/CsOH/H_2O system, indicating that some vesicles became larger, and only half of the vesicle edges can be observed [68]. In addition, Cryo-TEM also enables us to build a 3D image of complex proteins or nanomaterials at incredible resolution [69].

Freeze-fracture TEM (FF-TEM) is one of the traditional methods based on initial cryofixation of the specimen. Unlike high-resolution EM imaging techniques, FF-TEM is mainly used in low- and medium-resolution structural studies, whilst it is advantageous in the extraordinary tolerance of different materials (solid, liquid, suspension, etc.) and experimental conditions (composition, temperature, pressure etc.) that may be an auxiliary in different researches. In a recent report, the aggregation and rheological behavior of vesicles formed by perfluorononanoic acid/NaOH was investigated using FF-TEM, and the formation of spherical unilamellar vesicles was demonstrated (Fig. 6f) [70].

To sum up, electron microscopy can provide high-resolution imaging although complicated sample pretreatments and strict working conditions may be required. Since soft organic materials do not give enough image contrasts, extra sample preparation techniques such as negative staining and freeze-fracture technique are normally required, which can produce undesired artifacts to EM images. The emergence of cryo-TEM allows the EM imaging under hydrated state, which can relatively avoid sample damage or distortion.

6. Scanning probe microscopy

Compared with LM and EM, scanning probe microscopy (SPM) has the advantages such as adaptable working environment, low sample damage, real-time and high-resolution imaging, as well as 3D imaging. Scanning probe microscopies are instrumental for studying surfaces at the nanoscale level. SPMs form images of surfaces using a physical probe that touches the surface of a sample to scan the surface and collect data, typically obtained as a two-dimensional grid of data points and displayed as a computer image. A variety of different probes and detection

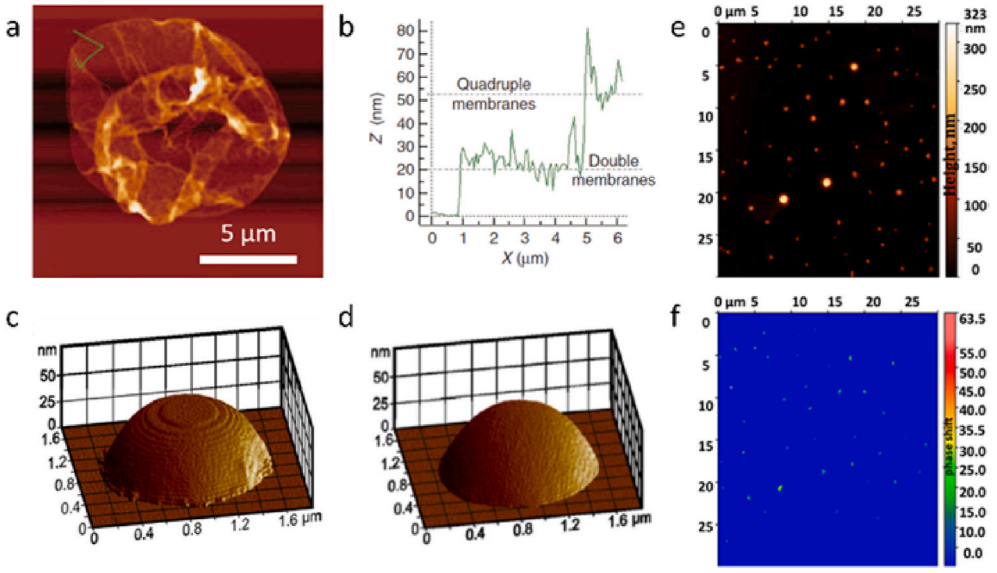

Fig. 7. (**a**) AFM image of a proteinosome dried on the substrate and (**b**) corresponding height profile along the green trace (upper, left corner) that traverses both double and quadruple membrane thicknesses associated with the collapsed/folded sample. (**c,d**) 3D AFM images of a single air-dried coacervate microdroplet composed of trans-azo TAB and PAA (**c**) in the dark and (d) under *in situ* UV irradiation. The trans-to-cis azobenzene conformational change leads to photo-induced loss of surface texture. (**e**) AFM and (**f**) MFM images of magnetic liposomes illustrating the efficient incorporation of magnetic nanoparticles on liposomes.

modalities can be used to generate either a surface topological map or to detect and image electromagnetic, physical or molecular properties, and the resultant technologies correspond to atomic force microscope (AFM), magnetic force microscope (MFM) and electrostatic force microscopy (EFM).

AFM is a surface influential analysis technique and can be used to obtain high-resolution nanoscale images with specimen in air (conventional AFM) or liquid (electrochemical AFM) environments. The critical part of AFM is an atomic sharp tip of approximately 10–20 nm in diameter sitting at the end of a cantilever. The tip moves in response to tip-surface interactions, and this movement is recorded by focusing a laser beam with a photodiode. The atom at the apex of the tip 'senses' individual atoms on the underlying sample surface when it forms incipient chemical bonds with each atom. Because these interactions delicately alter the tip's vibration frequency, the sample surface can be detected and mapped. Hence, the imaging can be realized by measuring the height changes of scanning points, and the detection of atoms on a variety of surfaces can also be achieved. For instance, proteinosome system was constructed by the interfacial assembly of BSA-NH_2/PNIPAAm nano-conjugates has ultrathin membrane of *ca.* 10 nm by AFM (Fig. 7a and b) [71]. Given that the theoretical extended length of nano-conjugate is around 9 nm, this result suggested that the membrane is composed of single layer of BSA-NH_2/PNIPAAm nano-conjugate.

AFM can also provide high lateral resolution and true 3D image of the sample surface, which becomes a powerful tool for the cross-sectional measurements. For example, AFM was previously applied to study a light-responsive multipodal polyelectrolyte-surfactant micro-architecture composed of trans-azobenzene trimethylammonium bromide (trans-azoTAB) and polyacrylic acid (PAA). AFM results revealed dynamic shaping and self-division under light irradiation. The UV-induced melting and self-division of azoTAB:PAA mesophases were studied by 3D AFM imaging, showing that the melting process was accompanied by a loss of surface texture (Fig. 7c and d) [72].

For magnetic samples, MFM with magnetic probes offers the best choice, which can detect the interaction and reconstruct the surface magnetic structure. For example, a group of magnetic PEGylated liposomes are prepared for drug release, and AFM as well as MFM were applied to reveal the ratio of magnetic liposomes [73]. By comparing the height information of liposomes by AFM tapping mode and the corresponding phase shift due to magnetic interactions by MFM, the collaborative results (Fig. 7e and f) suggested that there is less than 30% of liposomes incorporating the magnetic nanoparticles.

7. Conclusions and perspectives

To date, protocells constructed from bottom-up approaches have exhibited great significance in exploring the origin of life and the construction of adaptive materials. In general, BFM is a good start for most protocell imaging since it is easy to access for most chemistry labs. DFM (or PCM) and PLM can be applied to acquire some fine details or birefringent phenomenon existing in samples. CLSM is excellent for out-of-focus light elimination and 3D image. For membrane imaging or details within a few hundred nanometers of the coverslip in protocells, SRM and TIRFM can be a good option. When further high-resolution imaging is required, EM remains the first choice, in which Cryo-EM or FF-TEM may be preferred to avoid imaging artifacts. Finally, AFM is the only technique that can measure samples submerged in a liquid. This is especially useful for in-situ characterization of protocol behaviours.

To conclude, the develop of advanced microscopy techniques by integrating computer-assisted soft tool or data analysis will greatly benefit the in-depth study of protocell, and thereby shedding light on the origin of life and the development of integrated constructs for diverse procedures in synthetic biology.

Author statement

The contents of this manuscript have not been published by any of the authors nor are they under consideration for publication in any other journals at the time of submission.

Declaration of competing interest

The authors declare no conflict of Interest.

Acknowledgements

This work was financially supported by the National Natural Science Foundation of China (Number 22072159).

References

[1] A.J. Dzieciol, S. Mann, Designs for life: protocell models in the laboratory, Chem. Soc. Rev. 41 (2012) 79–85.
[2] Z. Nourian, C. Danelon, Linking genotype and phenotype in protein synthesizing liposomes with external supply of resources, ACS Synth. Biol. 2 (2013) 186–193.

[3] X. Liu, P. Formanek, B. Voit, D. Appelhans, Functional cellular mimics for the spatiotemporal control of multiple enzymatic cascade reactions, Angew. Chem. Int. Ed. 56 (2017) 16233–16238.
[4] X. Huang, A.J. Patil, M. Li, S. Mann, Design and construction of higher-order structure and function in proteinosome-based protocells, J. Am. Chem. Soc. 136 (2014) 9225–9234.
[5] A.D. Dinsmore, M.F. Hsu, M.G. Nikolaides, M. Marquez, A.R. Bausch, D.A. Weitz, Colloidosomes: selectively permeable capsules composed of colloidal particles, Science 298 (2002) 1006–1009.
[6] S. Koga, D.S. Williams, A.W. Perriman, S. Mann, Peptide–nucleotide microdroplets as a step towards a membrane-free protocell model, Nat. Chem. 3 (2011) 720–724.
[7] P. Wen, X. Liu, L. Wang, M. Li, Y.D. Huang, X. Huang, S. Mann, Coordinated membrane dusion of proteinosomes by contact-Induced hydrogel self-Healing, Small 13 (2017) 1700467.
[8] A.F. Mason, N.A. Yewdall, P.L.W. Welzen, J.X. Shao, M.V. Stevendaal, J.C.M. V. Hest, D.S. Williams, L.K.E.A. Abdelmohsen, Mimicking cellular compartmentalization in a hierarchical protocell through spontaneous spatial organization, ACS Cent. Sci. 5 (2019) 1360–1365.
[9] P. Gobbo, A.J. Patil, M. Li, R. Harniman, W.H. Briscoe, S. Mann, Programmed assembly of synthetic protocells into thermoresponsive prototissues, Nat. Mater. 17 (2018) 1145–1153.
[10] D.J. Stephens, V.J. Allan, Light microscopy techniques for live cell imaging, Science 300 (2003) 82–86.
[11] B. Amos, Lessons from the history of light microscopy, Nat. Cell Biol. 2 (2000) E151–E152.
[12] H. Wang, X. Zhu, L. Tsarkova, A. Pich, M. Moller, All-silica colloidosomes with a particle-bilayer shell, ACS Nano 5 (2011) 3937–3942.
[13] M. Li, D.C. Green, J.L.R. Anderson, B.P. Binks, S. Mann, In vitro gene expression and enzyme catalysis in bio-inorganic protocells, Chem. Sci. 2 (2011) 1739–1745.
[14] M. Li, X. Huang, S. Mann, Spontaneous growth and division in self-reproducing inorganic colloidosomes, Small 10 (2014) 3291–3298.
[15] C. Wu, S. Bai, M.B. Ansorge-Schumacher, D.Y. Wang, Nanoparticle cages for enzyme catalysis in organic media, Adv. Mater. 23 (2011) 5694–5699.
[16] M. Li, R.L. Harbron, J.V.M. Weaver, B.P. Binks, S. Mann, Electrostatically gated membrane permeability in inorganic protocells, Nat. Chem. 5 (2013) 529.
[17] L. Rodríguez-Arco, M. Li, S. Mann, Phagocytosis-inspired behaviour in synthetic protocell communities of compartmentalized colloidal objects, Nat. Mater. 16 (2017) 857–863.
[18] H. Ueno, S. Nishikawa, R. Iino, K.V. Tabata, S. Sakakihara, T. Yanagida, H. Noji, Simple dark-field microscopy with nanometer spatial precision and microsecond temporal resolution, Biophys. J. 98 (2010) 2014–2023.
[19] P. Gobbo, L. Tian, B.V.V.S.P. Kumar, S. Turvey, M. Cattelan, A.J. Patil, M. Carraro, M. Bonchio, S. Mann, Catalytic processing in ruthenium-based polyoxometalate coacervate protocells, Nat. Commun. 11 (2020) 1–9.
[20] S.Y. Sun, M. Li, F. Dong, S.J. Wang, L.F. Tian, S. Mann, Chemical signaling and functional activation in colloidosome-based protocells, Small 12 (2016) 1920–1927.
[21] D.S. Williams, A.J. Patil, S. Mann, Spontaneous structuration in coacervate-based protocells by polyoxometalate-mediated membrane assembly, Small 10 (2014) 1830–1840.
[22] K. Kurihara, M. Tamura, K. Shohda, T. Toyota, K.T. Suzuki, T.D. Sugawara, Self-reproduction of supramolecular giant vesicles combined with the amplification of encapsulated DNA, Nat. Chem. 3 (2011) 775.
[23] C.I. McPhee, G. Zoriniants, W. Langbein, P. Borri, Measuring the lamellarity of giant lipid vesicles with differential interference contrast microscopy, Biophys. J. 105 (2013) 1414–1420.
[24] M. Srinivasarao, G.S. Iannacchione, A.N. Parikh, Biologically inspired far-from-equilibrium materials, MRS Bull. 44 (2019) 91–95.
[25] T.Y.D. Tang, C.R.C. Hak, A.J. Thompson, M.K. Kuimova, D.S. Williams, A. W. Perriman, S. Mann, Fatty acid membrane assembly on coacervate microdroplets as a step towards a hybrid protocell model, Nat. Chem. 6 (2014) 527.
[26] I.A. Chen, K. Salehi-Ashtiani, J.W. Szostak, RNA catalysis in model protocell vesicles, J. Am. Chem. Soc. 127 (2005) 13213–13219.
[27] T.Y.D. Tang, D. Cecchi, G. Fracasso, D. Accardi, A. Coutable-Pennarun, S.S. Mansy, A.W. Perriman, J.L.R. Anderson, S. Mann, Gene-mediated chemical communication in synthetic protocell communities, ACS Synth. Biol. 7 (2018) 339–346.
[28] P. Gao, G.U. Nienhaus, Confocal laser scanning microscopy with spatiotemporal structured illumination, Opt. Lett. 41 (2016) 1193–1196.
[29] B.P. Kumar, J. Fothergill, J. Bretherton, L.F. Tian, A.J. Patil, S.A. Davis, S. Mann, Chloroplast-containing coacervate micro-droplets as a step towards photosynthetically active membrane-free protocells, Chem. Commun. 54 (2018) 3594–3597.
[30] Y. Yin, L. Niu, X. Zhu, M.P. Zhao, Z.X. Zhang, S. Mann, D.H. Liang, Non-equilibrium behaviour in coacervate-based protocells under electric-field-induced excitation, Nat. Commun. 7 (2016) 1–7.
[31] N. Martin, J.P. Douliez, Y. Qiao, R. Booth, M. Li, S. Mann, Antagonistic chemical coupling in self-reconfigurable host–guest protocells, Nat. Commun. 9 (2018) 1–12.
[32] D.R. Miller, J.W. Jarrett, A.M. Hassan, A.K. Dunn, Deep tissue imaging with multiphoton fluorescence microscopy, Curr. Opin. Biomed. Eng. 4 (2017) 32–39.
[33] N.G. Horton, K. Wang, D. Kobat, C.G. Clark, F.W. Wise, C.B. Schaffer, C. Xu, In vivo three-photon microscopy of subcortical structures within an intact mouse brain, Nat. Photon. 7 (2013) 205–209.
[34] F. Helmchen, W. Denk, Deep tissue two-photon microscopy, Nat. Methods 2 (2005) 932–940.
[35] F. Schueder, J. Lara-Gutiérrez, B.J. Beliveau, S.K. Saka, H.M. Sasaki, J. B. Woehrstein, M.T. Strauss, H. Grabmayr, P. Yin, R. Jungmann, Multiplexed 3D super-resolution imaging of whole cells using spinning disk confocal microscopy and DNA-PAINT, Nat. Commun. 8 (2017) 1–9.
[36] R. Montecchi, E. Schwob, Long-term imaging of DNA damage and cell cycle progression in budding yeast using spinning disk confocal microscopy, Genome Instability 1672 (2018) 527–536.
[37] O. Gershony, S. Sherman, S. Adar, I. Segal, D. Nachmias, I. Goliand, N. Elia, Measuring abscission spatiotemporal dynamics using quantitative high-resolution microscopy, Methods Cell Biol. 137 (2017) 205–224.
[38] B. Zobiak, A.V. Failla, Advanced spinning disk-TIRF microscopy for faster imaging of the cell interior and the plasma membrane, J. Microsc. 269 (2018) 282–290.
[39] T. Lu, E. Spruijt, Multiphase complex coacervate droplets, J. Am. Chem. Soc. 142 (2020) 2905–2914.
[40] Y. Wu, P. Wawrzusin, J. Senseney, R.S. Fischer, R. Christensen, A. Santella, A. G. York, P.W. Winter, C.M. Waterman, Z.R. Bao, D.A. Colón-Ramos, M. McAuliffe, H. Shroff, Spatially isotropic four-dimensional imaging with dual-view plane illumination microscopy, Nat. Biotechnol. 31 (2013) 1032–1038.
[41] K. Becker, S. Saghafi, M. Pende, Inna Sabdyusheva-Litschauer, C.M. Hahn, M. Foroughipour, N. Jährling, H. Dodt, Deconvolution of light sheet microscopy recordings, Sci. Rep. 9 (2019) 1–14.
[42] G. Vicidomini, P. Bianchini, A. Diaspro, STED super-resolved microscopy, Nat. Methods 15 (2018) 173.
[43] S.T. Hess, T.P.K. Girirajan, M.D. Mason, Ultra-high resolution imaging by fluorescence photoactivation localization microscopy, Biophys. J. 91 (2006) 4258–4272.
[44] S.H. Lee, J.Y. Shin, A. Lee, C. Bustamante, Counting single photoactivatable fluorescent molecules by photoactivated localization microscopy (PALM), Proc. Natl. Acad. Sci. Unit. States Am. 109 (2012) 17436–17441.
[45] H. Blom, J. Widengren, Stimulated emission depletion microscopy, Chem. Rev. 117 (2017) 7377–7427.
[46] Y. Wu, H. Shroff, Faster, sharper, and deeper: structured illumination microscopy for biological imaging, Nat. Methods 15 (2018) 1011–1019.
[47] K. Hu, L. Ji, K.T. Applegate, G. Danuser, C.M. Waterman-Storer, Differential transmission of actin motion within focal adhesions, Science 315 (2007) 111–115.
[48] A. Demuro, I. Parker, Imaging single-channel calcium microdomains by total internal reflection microscopy, Biol. Res. 37 (2004) 675–679.
[49] G. Vizcay-Barrena, S.E. D Webb, M.L. Martin-Fernandez, Z.A. Wilson, Subcellular and single-molecule imaging of plant fluorescent proteins using total internal reflection fluorescence microscopy (TIRFM), J. Exp. Bot. 62 (2011) 5419–5428.
[50] A.J. Heron, J.R. Thompson, A.E. Mason, M.I. Wallace, Direct detection of membrane channels from gels using water-in-oil droplet bilayers, J. Am. Chem. Soc. 129 (2007) 16042–16047.
[51] M.C. Huber, A. Schreiber, P. Von Olshausen, B.R. Varga, O. Kretz, B. Joch, S. Barnert, R. Schubert, S. Eimer, P. Kele, S.M. Schiller, Designer amphiphilic proteins as building blocks for the intracellular formation of organelle-like compartments, Nat. Mater. 14 (2015) 125–132.
[52] Y. Qiao, M. Li, R. Booth, S. Mann, Predatory behaviour in synthetic protocell communities, Nat. Chem. 9 (2017) 110–119.
[53] S. Roy, S. Mandal, P. Banerjee, N. Sarkar, Modification of fatty acid vesicle using an imidazolium-based surface-active ionic liquid: a detailed study on its modified properties using spectroscopy and microscopy techniques, J. Chem. Sci. 130 (2018) 132.
[54] B. Drobot, J.M. Iglesias-Artola, K. Le Vay, V. Mayr, M. Kar, M. Kreysing, H. Mutschler, T.-Y.D. Tang, Compartmentalised RNA catalysis in membrane-free coacervate protocells, Nat. Commun. 9 (2018) 1–9.
[55] S. Villringer, J. Madl, T. Sych, C. Manner, A. Imberty, W. Römer, Lectin-mediated protocell crosslinking to mimic cell-cell junctions and adhesion, Sci. Rep. 8 (2018) 1–11.
[56] F. Pir Cakmak, A.T. Grigas, C.D. Keating, Lipid vesicle-coated complex coacervates, Langmuir 35 (2019) 7830–7840.
[57] B.S. Schuster, E.H. Reed, R. Parthasarathy, C.N. Jahnke, R.M. Caldwell, J. G. Bermudez, H. Ramage, M.C. Good, D.A. Hammer, Controllable protein phase separation and modular recruitment to form responsive membraneless organelles, Nat. Commun. 9 (2018) 1–12.
[58] A. Beghin, A. Kechkar, C. Butler, F. Levet, M. Cabillic, O. Rossier, G. Giannone, R. Galland, D. Choquet, J.-B. Sibarita, Localization-based super-resolution imaging meets high-content screening, Nat. Methods 14 (2017) 1184–1190.
[59] R.K. Kumar, X. Yu, A.J. Patil, M. Li, S. Mann, Cytoskeletal-like supramolecular assembly and nanoparticle-based motors in a model protocell, Angew. Chem. Int. Ed. 123 (2011) 9515–9519.
[60] Q.L. Zou, L. Zhang, X.H. Yan, A.H. Wang, G.H. Ma, J.B. Li, H. Mçhwald, S. Mann, Multifunctional porous microspheres based on peptide-porphyrin hierarchical Co-assembly, Angew. Chem. Int. Ed. 126 (2014) 2398–2402.
[61] C. Zhao, M. Zhu, Y. Fang, X.M. Liu, L. Wang, D.F. Chen, X. Huang, Engineering proteinosomes with renewable predatory behaviour towards living organisms, Mater. Horizons. 7 (2020) 157–163.
[62] G. Wu, L. Wang, P. Zhou, P. Wen, C. Ma, X. Huang, Y.D. Huang, Design and construction of hybrid microcapsules with higher-order structure and multiple functions, Adv. Sci. 5 (2018) 1700460.
[63] R.W. Jaggers, R. Chen, S.A.F. Bon, Control of vesicle membrane permeability with catalytic particles, Mater. Horizons. 3 (2016) 41–46.
[64] W. Denk, H. Horstmann, Serial block-face scanning electron microscopy to reconstruct three-dimensional tissue nanostructure, PLoS Biol. 2 (2004) e329.
[65] K.J. Hayworth, J.L. Morgan, R. Schalek, D.R. Berger, D.G.C. Hildebrand, J. W. Lichtman, Imaging ATUM ultrathin section libraries with WaferMapper: a

multi-scale approach to EM reconstruction of neural circuits, Front. Neural Circ. 8 (2014) 68.
[66] X.M. Liu, P. Zhou, Y.D. Huang, M. Li, X. Huang, S. Mann, Hierarchical proteinosomes for programmed release of multiple components, Angew. Chem. Int. Ed. 128 (2016) 7211–7216.
[67] N. Du, R.Y. Song, H.P. Li, S. Song, R.J. Zhang, W.G. Hou, A nonconventional model of protocell-like vesicles: anionic clay surface-mediated formation from a single-tailed amphiphile, Langmuir 31 (2015) 12579–12586.
[68] W. Xu, A. Song, S. Dong, J.F. Chen, J.C. Hao, A systematic investigation and insight into the formation mechanism of bilayers of fatty acid/soap mixtures in aqueous solutions, Langmuir 29 (2013) 12380–12388.
[69] M.J.M. Wirix, P.H.H. Bomans, H. Friedrich, N.A.J.M. Sommerdijk, G.D. With, Three-dimensional structure of P3HT assemblies in organic solvents revealed by cryo-TEM, Nano Lett. 14 (2014) 2033–2038.
[70] J. Zhang, G. Xu, A. Song, L. Wang, M.Q. Lin, Z.X. Dong, Z.H. Yang, Faceted fatty acid vesicles formed from single-tailed perfluorinated surfactants, Soft Matter 11 (2015) 7143–7150.
[71] X. Huang, M. Li, D.C. Green, D.S. Williams, A.J. Patil, S. Mann, Interfacial assembly of protein–polymer nano-conjugates into stimulus-responsive biomimetic protocells, Nat. Commun. 4 (2013) 1–9.
[72] N. Martin, K.P. Sharma, R.L. Harniman, R.M. Richardson, R.J. Hutchings, D. Alibhai, M. Li, S. Mann, Light-induced dynamic shaping and self-division of multipodal polyelectrolyte-surfactant microarchitectures via azobenzene photomechanics, Sci. Rep. 7 (2017) 1–12.
[73] K.Y. Vlasova, A. Piroyan, I.M. Le-Deygen, H.M. Vishwasrao, J.D. Ramsey, N. L. Klyachko, Y.I. Golovin, P.G. Rudakovskaya, I.I. Kireev, A.V. Kabanov, M. Sokolsky-Papkov, Magnetic liposome design for drug release systems responsive to super-low frequency alternating current magnetic field (AC MF), J. Colloid Interface Sci. 552 (2019) 689–700.